Investigation of Intermediates and Transition States in the Catalytic Mechanisms of Active Site Substituted Cobalt(II), Nickel(II), Zinc(II), and Cadmium(II) Horse Liver Alcohol Dehydrogenase†

Michael F. Dunn,* Helmut Dietrich,‡ Alastair K. H. MacGibbon,§ Steven C. Koerber,‖ and Michael Zeppezauer*

ABSTRACT: The active site substituted Co(II)-, Ni(II)-, and Cd(II)-horse liver alcohol dehydrogenase derivatives are compared to the native Zn(II)-enzyme with respect to the kinetic properties associated with the formation and decay of the intermediate observed in the reaction of the binary E-(NADH) complex with the intense substrate chromophore *trans*-4-(*N*,*N*-dimethylamino)cinnamaldehyde (DACA), λ_{max} 398 nm (H_2O). Previous studies with this chromophore and the native Zn(II)-enzyme [Morris, R. G., Saliman, G., & Dunn, M. F. (1980) *Biochemistry 19*, 725; Dunn, M. F., Biellmann, J.-F., & Branlant, G. (1975) *Biochemistry 14*, 3176] have established that the red-shifted spectrum of the intermediate (λ_{max} 464 nm) is due to inner-sphere coordination of the carbonyl oxygen of DACA to the active-site zinc of the enzyme. In the present work, all the metal ion substituted enzymes were found to form intermediates with red-shifted spectra upon reaction with DACA and NADH. The magnitudes of (1) the red shifts, (2) the specific rate constants (k_{off}) for dissociation of DACA from the intermediate, and (3) the hydride transfer rate constants (k_H) were found to correlate with the expected order of the Lewis acid acidities (assuming tetrahedral coordination); i.e., Co(II) > Ni(II) ≥ Zn(II) ≫ Cd(II). The k_H value for the Co(II)-E was found to be 1.4-fold greater than the value of 7.2 s^{-1} for Zn(II)-E, while the Cd-(II)-E was 40-fold lower. The kinetic isotope effect on k_H upon replacement of the (4*R*)-4-hydrogen of NADH by deuterium was found to be similar for the Co(II)-, Ni(II)-, and Zn-(II)-enzymes ($k_H/k_D \simeq 3.0$) but somewhat lower for the Cd(II)-enzyme ($k_H/k_D \simeq 1.7$). The apparent ionization constants (pK_{app}) for the pH-dependent decay of the DACA intermediate ranged from about 5.5 to 7 but are dependent on both the nature of the active site metal ion and the substitution of the (4*R*)-4-hydrogen of NADH by deuterium, indicating that pK_{app} is a complex term. Investigation of the visible spectral changes for the intermediate decay with the Co(II)-enzyme species via rapid scanning spectrophotometry demonstrated that the disappearance of the DACA chromophore to products and changes in the Co(II) d–d absorption bands are concomitant processes. We conclude that the close similarities in kinetic properties exhibited by Co(II)-, Ni(II)-, and Zn(II)-enzymes arise from the close similarities in coordination geometries and Lewis acid strengths which lead to highly similar transition states for the processes of intermediate formation and decay. The 40-fold lower reactivity and smaller kinetic isotope effect exhibited by the Cd(II)-enzyme are proposed to be a consequence of several interrelated factors: (1) a lower Lewis acid strength, (2) longer bonds to Cd(II) which result in misalignment of the reacting atoms, and (3) perhaps a different coordination number and/or geometry.

The replacement of the active-site zinc ions of equine liver alcohol dehydrogenase (LADH)[1] by other divalent metal ions is of considerable experimental and theoretical relevance to the investigation of catalytic mechanism. The substitution of Co(II) and Cd(II), although difficult, has been accomplished by several groups to give a variety of enzyme species. Enzyme species derived from the replacement of all four zinc ions per dimer, and species derived from replacement of either the two active-site zinc ions or the two "structural" zinc ions have been prepared. [For examples, see Drum & Vallee (1970), Shore & Santiago (1975), Sytkowski & Vallee (1978), and Maret et al. (1979)].

Maret et al. (1979) have shown that the active-site zinc ions can be selectively removed from LADH crystals without significant changes in the zinc occupancy of the structural sites. The resulting inactive species (apoenzyme) can be reconstituted to the native enzyme in high yield with full recovery of activity. Under slightly differing conditions, the apoenzyme crystals can be active site specifically reconstituted with Co(II) (Maret et al., 1979), Ni(II) (Dietrich et al., 1981), Cd(II) (Andersson, 1980), and Cu(II) (Maret et al., 1979).

Previous studies of the various metal ion substituted enzyme derivatives have focused on the characterization of (a) the spectroscopic properties (i.e., UV–visible, fluorescence, circular dichroism, ^{113}Cd NMR, and ESR spectra) [see above references, Bobsein & Myers (1979), and Dietrich et al. (1979)], (b) the investigation of the kinetics of metal ion exchange, and (c) the effects of both reversibly bound and covalently attached inhibitors on the spectral properties of the derivatives. Shore & Santiago (1975) have reported that the rate of hydride transfer in the oxidation of ethanol is significantly slower for

† From the Fachbereich Analytische und Biologische Chemie, Universität des Saarlandes, D-6600 Saarbrücken, West Germany, and Department of Biochemistry, University of California, Riverside, Riverside, California 92521. *Received March 10, 1981.* This work was supported by National Science Foundation Grant No. PCM-7911526, Grant No. Ze 152/7 of the Deutsche Forschungsgemeinschaft, and the Fonds der Chemischen Industrie.

‡ Present address: Institut für Weinchemie und Getränketechnologie, Forschungsanstalt Geisenheim, 6222 Geisenheim, West Germany.

§ Present address: Department of Chemistry, Biochemistry and Biophysics, Massey University, Palmerston North, New Zealand.

‖ Present address: Division of Natural Sciences, University of California, Santa Cruz, CA 95064.

[1] Abbreviations used: LADH, Zn(II)-E, or E, native horse liver alcohol dehydrogenase (EC 1.1.1.1); Co(II)-, Ni(II)-, and Cd(II)-E, the cobalt, nickel, and cadmium specific active site substituted enzyme derivatives; apoenzyme or apo-E, enzyme lacking metal ion at the active site; NAD^+ and NADH, oxidized and reduced nicotinamide adenine dinucleotide; NADD, (4*R*)-4-deuterio-NADH; DACA, *trans*-4-(*N*,*N*-dimethylamino)cinnamaldehyde; pyr, pyrazole; H_2NADH, reduced 1,4,5,6-tetrahydronicotinamide adenine dinucleotide.

0006-2960/82/0421-0354$01.25/0

Scheme I

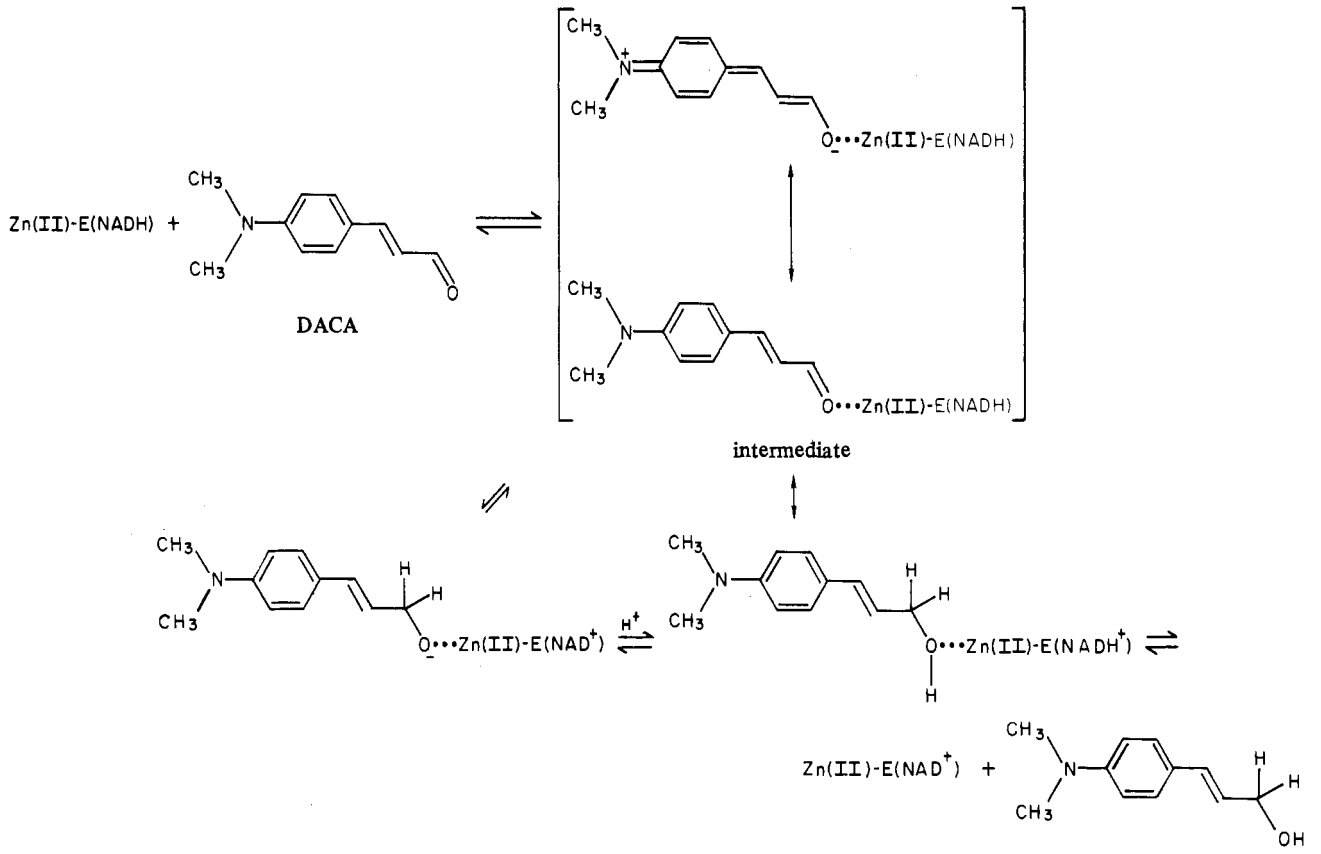

totally Co(II)-substituted enzyme than for native enzyme. Although the Co(II)- and Cd(II)-enzymes have been shown to be catalytically active, no detailed mechanistic studies of the catalytic mechanism have been published.

The new methods for preparing enzyme derivatives with only the active-site zinc ions replaced (Maret et al., 1979) in combination with rapid kinetic techniques have provided us with the unique opportunity to probe the effects of metal ion substitution on both intermediates and transition states in the LADH catalytic mechanism. As we shall show in this and subsequent papers, the substitution of Co(II), Ni(II), and Cd(II) for the active-site zinc ions provides a chemically and structurally subtle means for modifying the catalytic properties of the enzyme. Since only the active-site metal is replaced, comparisons among these derivatives reflect solely the structural and electronic effects of the catalytic metal ion. These studies provide new insight as to how intermediates and transition states along the reaction path are influenced by what we presume to be small changes in bond lengths (<0.3 Å), bond angles, and charge density on the metal ion.

Here we report the metal ion dependencies of pH effects and deuterium kinetic isotope effects for Co(II)-, Ni(II)- and Cd(II)-substituted LADH on the formation and decay of the chemical intermediate observed in the reduction of *trans*-4-(*N*,*N*-dimethylamino)cinnamaldehyde (DACA). This intermediate is characterized by a large red shift in the UV–visible spectrum of the DACA chromophore (from 398 to 464 nm in the zinc enzyme). Previous studies have shown the intermediate to have a structure involving inner-sphere coordination of the carbonyl oxygen of DACA to zinc (or cobalt) ion at the LADH active sites (Dunn & Hutchison, 1973; Dunn et al., 1975; Angelis et al., 1977; Dietrich et al., 1979; Morris et al., 1980). These studies have led to the proposal that (1) zinc ion plays a Lewis acid catalytic role in activating the aldehyde carbonyl for attack by hydride, (2) reduced coenzyme plays a noncovalent effector role in the activation of aldehyde, (3) hydride transfer is not facilitated by a proton transfer prior to, or concerted with, hydride transfer, and (4) release of products from the site is triggered by proton transfer to the metal ion coordinated alcoholate ion (viz., Scheme I). This paper is the first in a series of reports from our laboratories describing detailed mechanistic investigations of Co(II)-, Ni(II)- and Cd(II)-substituted LADH. Subsequent papers will report the characterization of several new intermediates discovered while investigating the reactions of other substrates with the Co(II)-E(NADH) complex.

Experimental Procedures

Buffer solutions were prepared from crystalline salts by using doubly glass-distilled water. As chloride ion may interfere with coenzyme binding and dissociation steps (Sund & Theorell, 1963; Shore & Gutfreund, 1970), the buffers were kept as low in chloride ion concentration as practical (see below). NADH and NAD^+ were obtained from Sigma Chemical Co. or Boehringer Mannheim as the highest purity grades. Both the specifically labeled (4*R*)-4-deuterio-NADH (NADD) and the NADH used in the deuterium kinetic isotope studies were prepared by the method of Rafter & Colwick (1957) as modified by Dunn & Hutchison (1973). The coenzyme prepared via this procedure was further purified by the method of Silverstein (1965). The reagents DACA and pyrazole (Aldrich) were purified by vacuum sublimation prior to use.

The metal-substituted LADH derivatives were prepared from the crystalline native enzyme by the method of Maret et al. (1979). Substitution involved the selective replacement of the active-site zinc ions via diffusion of the appropriate metal ion (Co^{2+}, Ni^{2+}, or Cd^{2+}) into preparations of the crystalline enzyme which had been depleted of zinc ion at the catalytic sites (hereafter referred to as apoenzyme). Reconstitutions

of the metal-substituted derivatives from the apoenzyme were accomplished as previously described for the Co(II)-enzyme (Maret et al., 1979), the Ni(II)-enzyme (Dietrich et al., 1981), and the Cd(II)-enzyme (Andersson, 1980). The Cd(II)-enzyme was prepared by dialyzing the suspension of apoenzyme crystals against 0.025 M Tes buffer, pH 7.0, containing 1 mM Cd^{2+} in the presence of *tert*-butanol (25% v/v) for 12 h at 4 °C. All preparation, storage, and manipulation of enzyme solutions were carried out under a N_2 atmosphere to protect the enzyme derivatives from the oxidative effects of O_2.

The apoenzyme used in the preparation of Co(II)-enzyme, when assayed by the method of Dalziel (1957), was found to retain ≤5% activity which we attribute to residual zinc at the active sites. The apoenzyme used to prepare the Cd(II)- and Ni(II)-enzymes retained 0.7% residual activity. The metal ion substituted enzyme derivatives were assayed by using the procedures and extinction coefficients previously described for protein concentration, specific metal ion concentration, and NADH binding capacity (Maret et al., 1979; Dietrich, 1980; Andersson, 1980). Assays of the Co(II)- and Ni(II)-enzymes involved quantitative determination of three distinct features of each sample: (a) the protein concentration, determined from the absorbance at 280 nm and each specific extinction coefficient, (b) the specific metal ion content, determined spectroscopically by using an ϵ_{350} for Co(II)-E of 7000 M^{-1} cm^{-1} (per 80000 daltons) and an ϵ_{407} for Ni(II)-E of 7000 M^{-1} cm^{-1}, and (c) the total NADH binding capacity, measured by fluorometric titration of the sample with NADH in the presence of 30 mM isobutyramide. Note that both the Cd(II)-E and the apoenzyme were also assayed by protein 280-nm absorption and by the unique fluorescence properties of the ternary NADH–isobutyramide complexes. For the Cd(II)-E(NADH,IBA) complex, λ_{em} = 420 nm (λ_{ex} 330 nm) with Q_{410} = 18.2; for Cd(II)-E(NADH) with Q_{410} = 5.5; and for apo-E(NADH) λ_{em} = 415 nm, with Q_{410} = 5.2; Q_{410} refers to the ratios of fluorescence for bound and free NADH at 410 nm, respectively (Dietrich, 1980). Note that the fluorescence of the apo-E(NADH) complex is unaffected by isobutyramide. From these results the percentage of total protein which is metal substituted and the percentage of active sites as NADH binding sites which are metal substituted were determined. On the basis of the total protein concentration, the Co(II)-enzyme used in these experiments had at least 70% of the active sites substituted, the Ni(II)-enzyme 27%, and the Cd(II)-enzyme 50%. Except for the trace of Zn(II) remaining at the active sites, NADH binding titrations indicate the remainder of the protein primarily consisted of apoenzyme and traces of denatured enzyme (<3%). The derivatized enzyme crystals were dissolved in 0.2 M Tes buffer (pH 7.1) containing 0.15 M sodium chloride (added to facilitate dissolution). All concentrations of metal ion substituted enzyme reported herein refer to the concentrations of catalytically functional enzyme sites after mixing in the stopped-flow apparatus. The protein $E_{280}^{0.1\%}$ values used were Zn(II)-E, 0.455 mg^{-1} cm^2 (Dalziel, 1957); Co(II)-E, 0.49 mg^{-1} cm^2 (Maret et al., 1979); Ni(II)-E, 0.48 mg^{-1} cm^2 (Dietrich et al., 1981); Cd(II)-E, 0.5 mg^{-1} cm^2 (Dietrich, 1980); apoenzyme, 0.45 mg^{-1} cm^2 (Maret et al., 1979).

Those DACA experiments where the decay rates were slow (i.e., all decay studies with the Cd(II)-enzyme and all decay studies above pH 7.5) were recorded on a strip chart recorder attached to the stopped-flow instrument. The traces were graphically analyzed after subtracting, where necessary, any postburst steady-state turnover contributions (see Results). Transient kinetic studies were carried out and analyzed by using a computerized Durrum-Gibson Model D-110 stopped-flow spectrophotometer equipped with a Kel-F flow system and 2-cm light path. The characteristics of the computer system and data analysis program have been described previously (Dunn et al., 1979). The effect of pH on reaction rate was carried out via a "pH-jump" technique as previously described (Morris et al., 1980). Enzyme and NADH (or NADD) were premixed in dilute Tes buffer (pH 7.15) in one syringe and then mixed in the stopped-flow apparatus with DACA and pyrazole (20 mM) premixed in concentrated buffer (0.1 M) in the second syringe. The pH after mixing was determined by measuring the pH of a 1:1 mixture of the two buffers. The enzyme solution was prepared by dilution of concentrated stocks (200–600 μM) containing 0.2 M Tes (pH 7.15) and 0.15 M Cl^- into 4.5 mM Tes (pH 7.15) buffer. After the solution was mixed in the stopped-flow apparatus, the final concentration of Tes buffer and Cl^- were ≤3.15 and 0.75 mM, respectively.

Rate constants and amplitudes were determined by assuming that the time courses (corrected for any steady-state contributions) were single, first-order decays. In general, 100 μM DACA was sufficient to maximize the DACA decay rate. However, the extent to which rate saturation was attained was always checked by determining the decay rate for 50 μM DACA. At low pH, it was found necessary to measure decay rates at a series of DACA concentrations and then extrapolate to infinite concentration to determine the true maximum decay rate. Temperature perturbation of equilibrium (T-jump) measurements with the Cd(II)-enzyme were performed in the laboratory of Professor Dr. D. Riesner, Institut für Organische Chemie and Biochemie (Technische Hochschule Darmstadt, West Germany). The instrumentation has been previously described (Coutts et al., 1975). The kinetics of intermediate formation were determined in 0.1 M sodium pyrophosphate buffer (pH 9.60) by mixing equal molar amounts (0.98–98 μM) of DACA and Cd(II)-E(NADH) sites. The cell (2-mL volume) was initially thermostated to 20 °C. After a T jump to ~24 °C, the absorption changes at 460 nm were recorded. Data were analyzed as described under Results (Coutts et al., 1975).

Rapid-scan stopped-flow kinetic measurements were performed with a Princeton Applied Research 1412 photodiode array detector and LSI-11 based microprocessor data acquisition system (the PAR OMA-2) in combination with the Durrum D-110 stopped-flow apparatus. The details of this system have been described previously (Koerber & Dunn, 1981). In this application a quartz tungsten–iodide lamp was used as the source of "white" light. The scans (see Results) are uncorrected for stray light derived from the infrared region of the lamp spectrum. Therefore, the reported absorbance values are relative rather than true values.

Results

pH Dependence of Intermediate Decay. The rate of decay of the DACA intermediate was studied as a function of pH for each of the metal ion substituted enzyme derivatives. For simplification of the analysis of rates, the reaction was limited to a single turnover by including 20 mM pyrazole in the solution. Above pH 5.5, pyrazole is a potent inhibitor which quasi-irreversibly forms a complex with $E(NAD^+)$. At a concentration of 20 mM, the rate of complex formation is rapid with respect to the rate-determining step of the decay process, thus ensuring quantitative conversion of the intermediate to alcohol (Theorell & Yonetani, 1963; McFarland & Bernhard, 1972; Morris et al., 1980). While pyrazole is less effective below pH 5.5, the decay process is still characterized by a rapid

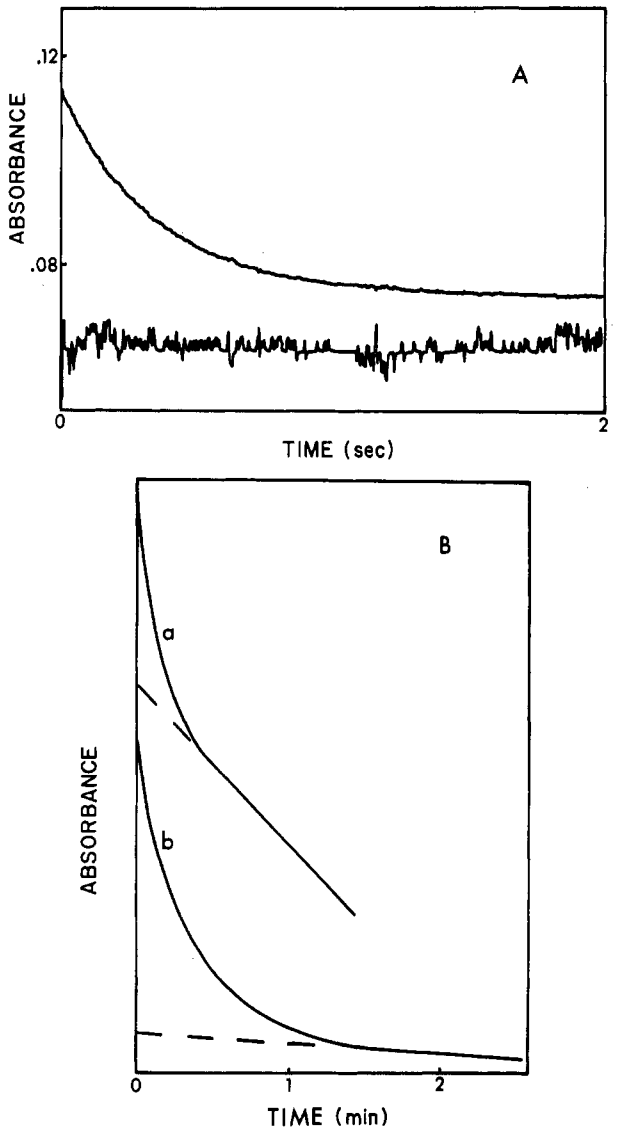

FIGURE 1: Time courses for intermediate decay with (A) Co(II)-substituted and (B) Cd(II)-substituted enzyme measured at 478 and 457 nm, respectively. Under the conditions employed, intermediate formation is essentially complete in the mixing dead time (~3 ms) of the stopped-flow apparatus and only the decay phase is observed. Conditions after mixing: (A) [Co(II)-E] = 1.68 μN; [NADH] = 91 μM; [DACA] = 97.1 μM; [pyr] = 20 mM; pH 5.99; 25.0 ± 0.2 °C. Computer best-fit parameters: k_{app} = 2.90 s^{-1}; amplitude = 0.0396 A; also shown is the difference between the theoretical and the observed trace, multiplied by a factor of 10. (B) [Cd(II)-E] = 1.5 μN; [NADH] = 100 μM; [DACA] = 100 μM; [pyr] = 20 mM; 25.0 ± 0.2 °C. Final pH values: trace a, pH 5.76; trace b, pH 7.45. Graphically analyzed rates: trace a, k_{app} = 0.125 s^{-1}; amplitude = 0.012 A; trace b, k_{app} = 0.0462 s^{-1}; amplitude = 0.016 A. The steady-state phases gave apparent turnover rates (v/[sites]) of 3.13 × 10^{-3} s^{-1} (trace a) and 2.0 × 10^{-4} s^{-1} (trace b).

burst but followed by a much slower steady-state recycling of the enzyme (Morris et al., 1980).

Figure 1A shows a typical decay time course for the intermediate with the Co(II)-enzyme measured at 478 nm, the absorption maximum for the intermediate. Similar time courses were observed for the Zn(II)-enzyme (Morris et al., 1980) and the Ni(II)-enzyme (data not shown). Figure 1B shows typical time courses at low and high pH for the Cd-(II)-enzyme. Note that at the high DACA concentration used, the intermediate forms within the mixing dead time of these stopped-flow experiments.

The decay time courses for the Co(II)-, Zn(II)- and Ni-(II)-enzymes, as judged by computer fitting of the data via a nonlinear least-squares reiterative method (Dunn et al., 1979), are well described by the equation for an apparent first-order process

$$A_t = A_\infty + Be^{-k_{app}t} \quad (1)$$

where A_t and A_∞ are respectively the absorbancies at times t and t_∞, B is the burst amplitude, and k_{app} is the observed rate constant. So that a visual impression of the goodness of fit could be provided, the best fit values of A_∞, B, and k_{app} from the computer analysis have been used to generate the theoretical time course. The difference between the theoretical trace and the observed trace is plotted in Figure 1A. As indicated by the pH independence of reaction amplitudes, the Zn(II)-, Co(II)- and Ni(II)-enzyme species yield a single turnover in the burst phase at all pH values studied (i.e., due to the effectiveness of pyrazole, the steady-state leakage is insignificant on the time scale of the decay reaction). However, the decay process for the Cd(II)-enzyme (Figure 1B) is much slower and therefore is perturbed by the steady-state leakage rate. Thus, the analysis of the decay phase is much more difficult for the Cd(II)-enzyme, and while the data in Figures 1B and 3 are qualitatively similar to those found for the other derivatives, the error in the determined rate constants does not allow a quantitative analysis of the pH dependence for the Cd(II)-enzyme. Since we observe the formation and decay of stoichiometric amounts of intermediate during a single turnover of sites (viz., Figures 1, 2, and 5), the 40-fold lower reactivity of the Cd(II)-enzyme (Figure 1 and Table I) must reflect the intrinsic effects of Cd(II) substitution for Zn(II); the lower reactivity cannot be due to trace amounts of contaminating active enzyme in an inactive preparation.

The rate of decay of the intermediate at saturating DACA concentration was determined as a function of pH for each metal ion derivative (Figures 2 and 3). The effects of deuterium substitution for the (4R)-4-hydrogen of NADH are also shown. The decay rate constants were found to display a remarkable range with pH. At high pH the rate constant is low and no kinetic isotope effect is observed (i.e., $k_H/k_D \simeq 1.0$). As the pH decreases, the rates increase and then approach a plateau where it will be noted that substitution of NADD for NADH yields a large kinetic isotope effect (Figures 2 and 3). For the Co(II)- and Ni(II)-enzymes $k_H/k_D \simeq 3.0$, a value similar to that found for the Zn(II)-enzyme. The apparent isotope effect for the Cd(II)-enzyme is smaller,

Table I: Summary of the Experimentally Derived Parameters for the Reaction of DACA with Metal Ion Substituted Enzyme Derivatives at 25.0 ± 2 °C

	Co(II)-E	Ni(II)-E	Zn(II)-E[a]	Cd(II)-E
k_H (s^{-1})	10.7	7.1	7.2	0.17[b]
k_H/k_D	2.9	3.1	2.8	1.7[b]
pK^H_{app} (±0.1)	5.5	6.1	6.0	
pK^D_{app} (±0.1)	6.1	6.7	6.5	
k_{off} (s^{-1})	80	110	180	380
k_{on} (M^{-1} s^{-1}) × 10^{-7}	2.0	1.6	4.0	2.5
$K_d = k_{off}/k_{on}$ (μM)[c]	4	7	7	15
λ_{max}[d]	478	475	464	457
$\Delta\lambda_{max}$[e]	80	77	66	59
E_T[f]	59.7	60.1	61.6	62.5

[a] Values for Zn(II)-E, the native enzyme, from Morris et al. (1980). [b] The k_H and k_H/k_D values for Cd(II)-E are estimates (see the text). [c] K_d is the kinetic equilibrium constant for DACA binding calculated from k_{off}/k_{on}. [d] λ_{max} refers to the absorption maximum of the DACA-E intermediate. [e] $\Delta\lambda_{max} = \lambda_{max}$(intermediate) − λ_{max}(free DACA), where the λ_{max} of free DACA is 398 nm in aqueous solution (pH 4–10). [f] Transition energies (kilocalories per mole of radiation).

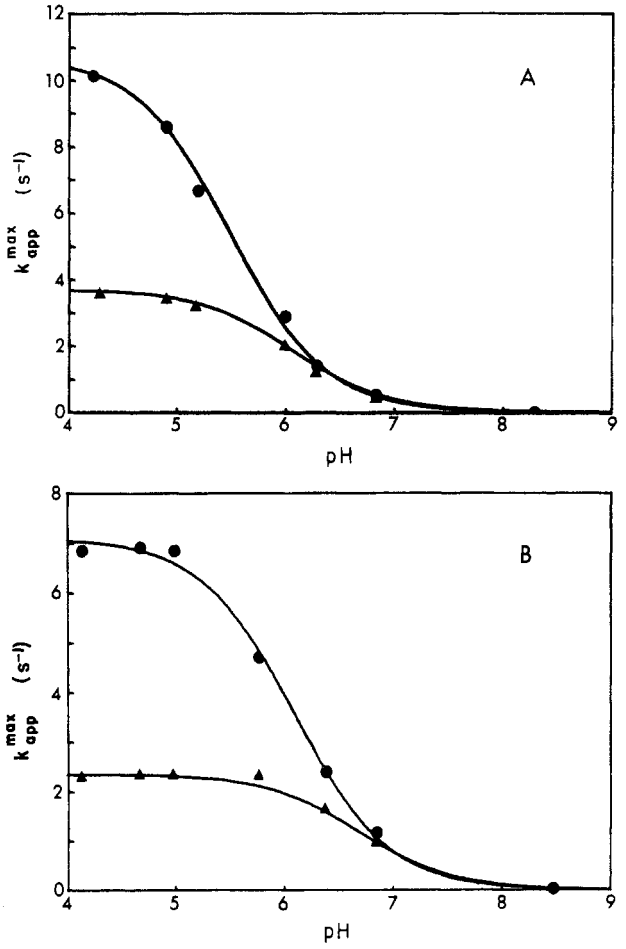

FIGURE 2: pH dependencies of the apparent decay rate constants k_{app}^{max} for the breakdown of the intermediates formed in the reactions of DACA with the Co(II)- and the Ni(II)-enzymes utilizing NADH (●) or NADD (▲) as the coenzyme. pH dependencies (A) for Co(II)-E and (B) for Ni(II)-E, both at 25.0 ± 0.2 °C. The buffers used and mixing conditions are described under Experimental Procedures. The solid lines in (A) and (B) are the best-fit lines when it is assumed that a single ionization is involved (see eq 2 of the text). Typical conditions are given in Figure 1 and the text (see Experimental Procedures and Results).

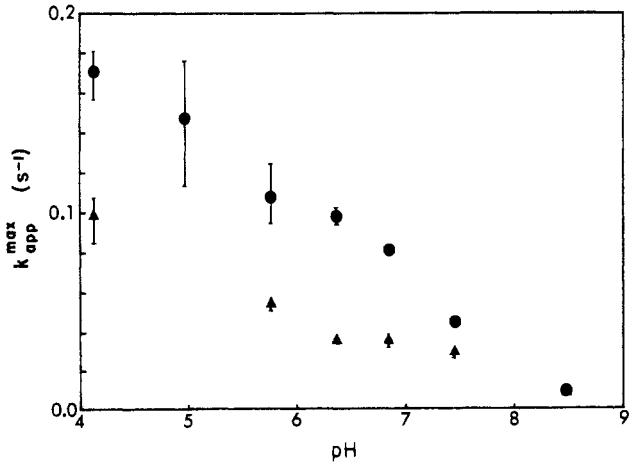

FIGURE 3: pH dependence of the apparent decay rate constants for the intermediate formed in the reaction of DACA with the Cd(II)-E at 25 ± 0.2 °C. See Figures 1 and 2 for typical conditions. The coenzyme used was NADH (●) or NADD (▲).

$k_H/k_D \sim 1.7$.

As previously found for the Zn(II)-E, the pH–rate profiles for the Co(II)- and Ni(II)-enzymes are well described by single

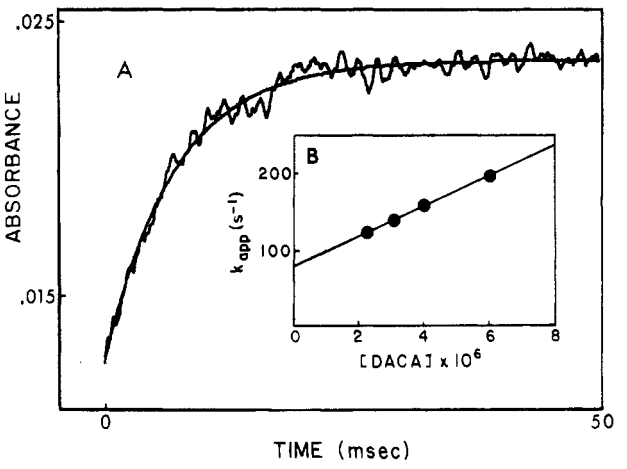

FIGURE 4: (A) Typical stopped-flow time course for the formation of the intermediate upon mixing DACA with the Co(II)-E(NADH) complex at 478 nm and 25.0 ± 0.2 °C. Conditions after mixing: [Co(II)-E] = 0.75 μN; [NADH] = 100 μM; [DACA] = 3.1 μM; final pH 6.80. The observed trace is overlaid with the theoretical time course from the computer best-fit parameters (assuming reaction is a pseudo-first-order process): k_{app} = 146 s^{-1}; amplitude = 0.014 A. (B) Dependence of k_{app} on [DACA]. Each data point represents the average value of at least three determinations. The solid line is the best fit (least squares) to the data points and yields values of (2.0 ± 0.2 × 10^7 M^{-1} s^{-1} and 80 ± 4 s^{-1} for the slope and intercept, respectively (viz., eq 4 of the text).

apparent ionization constants when a dependency of the form of eq 2 is assumed (solid line, Figure 2):

$$k_{app}^{max} = \frac{k_H[H^+]}{K_{app}^H + [H^+]} \quad (2)$$

K_{app}^H and k_H (or k_D for NADD) are the values obtained from the slope and intercept, respectively, of the plot of k_{app}^{max} vs. $k_{app}^{max}/[H^+]$ (Jencks, 1969). K_{app}^H or K_{app}^D is an apparent ionization constant and k_H (or k_D) is the pH-independent rate constant. The values of k_H, k_H/k_D, pK_{app}, and pK_{app}^D for the Co(II) and Ni(II) systems are given in Table I. Experimentally estimated rate constants are given for the Cd(II) system, while the Zn(II)-enzyme values are those reported by Morris et al. (1980). Repetition of these measurements for the Zn(II)-enzyme using the same buffers employed for the other derivatives gave virtually identical results with those previously published.

Because the data for the Ni(II)- and Zn(II)-enzymes in Table I are so similar, it was necessary to establish that the source of the observed changes was in fact due to the Ni(II) species and not due to changes from the small amount of Zn(II) contaminant (see Experimental Procedures). Therefore, the amplitudes of the decay process were measured for the Ni(II)-enzyme preparation at 475 and 464 nm, the respective λ_{max} values of the Ni(II)-E intermediate and the Zn(II)-E intermediate. The A_{475}/A_{464} ratio was found to be 1.4. This finding conclusively establishes that the spectral changes originate from the Ni(II)-substituted enzyme (Dietrich et al., 1981) and that there is very little contribution by Zn(II)-enzyme. Table I also presents for each derivative the specific association (k_{on}) and dissociation (k_{off}) rate constants for the reaction of DACA with the E(NADH) complex. The observed rate constants for the Co(II)- and Ni(II)-enzymes were slow enough to allow measurement via the stopped-flow rapid-mixing apparatus by measuring the rate of formation of the intermediate as a function of the concentration of DACA. In a typical experiment (Figure 4), Co(II)- or Ni(II)-enzyme (0.75 μN) and NADH (100 μM)

were preincubated and mixed in the stopped-flow apparatus with solutions of DACA (2.25–8 μM) in pH 6.8 phosphate buffer (0.05 M). (Concentrations refer to final values after mixing.) At these DACA concentrations the decay of the intermediate is so slow relative to the rate of intermediate formation that the decay phase could be ignored [see Dunn & Hutchison (1973)], yet the relatively high DACA concentrations used ensured pseudo-first-order behavior. These rate data were found to be well described by the simple, pseudo-first-order kinetic expression of eq 4 for the approach to equilibrium (eq 3), thus making possible the determination

$$\mathrm{E(NADH) + DACA} \underset{k_{off}}{\overset{k_{on}}{\rightleftharpoons}} \mathrm{intermediate} \qquad (3)$$

$$k_{app} = k_{off} + k_{on}[\mathrm{DACA}] \qquad (4)$$

of k_{on} and k_{off} from the slope and intercept, respectively, of plots of k_{app} vs. [DACA] (viz., Figure 4B).

For the faster rates of the Zn(II)-enzyme (Dunn & Hutchison, 1973) and the Cd(II)-enzyme, stopped-flow temperature-jump relaxation studies were carried out. The Cd(II) data were measured by using equal concentrations of enzyme sites and DACA in the range between 0.98 and 98.0 μM. The data were fit to eq 5 to obtain estimates of k_{on} and k_{off}.

$$(1/\tau)^2 = 4k_{on}k_{off}[\mathrm{DACA}]_0 + (k_{off})^2 \qquad (5)$$

Equation 5 is a special case of the relaxation expression for the bimolecular binding process described in eq 3 (Bernasconi, 1976) where τ is the experimentally observed relaxation time. The kinetically derived dissociation constants in Table I were calculated from the ratio k_{off}/k_{on}.

Rapid-scanning stopped-flow kinetic studies (Figure 5) were carried out with the Co(II)-enzyme to determine whether or not additional intermediates could be detected in the decay phase via changes in the Co(II)-enzyme d–d spectral bands. To allow simultaneous monitoring of the spectrum of the intermediate and the enzyme, the wavelength range 440–715 nm was scanned. Under the conditions used, the formation of the intermediate was too rapid to be followed with the rapid-scan detector. Thus, the background contributed by free DACA was constant throughout the series and all the intermediate was formed prior to the first scan. Consequently, the scans in Figure 5A record the spectral changes associated with the decay of the intermediate and the formation of the E-(NAD–pyrazole) complex. Since the decay process undergoes a pH-dependent change in the rate-limiting step (Figure 2A) from hydride transfer at low pH to some subsequent step at high pH, data sets were collected at both pH 4.4 and pH 6.85. Because the spectral changes were similar at each pH, only pH 4.4 data are shown. The important features of Figure 5 are as follows: (a) The intense absorbance at lowest wavelength is due to the large excess of free DACA (λ_{max} 398 nm). (b) The shoulder centered at 478 nm is due to the spectrum of the intermediate. This shoulder decays with the time course shown in Figure 5B. (c) Figure 5C shows an expansion of the spectral changes in the 540–715-nm region. Note that the first spectrum in the time course exhibits a single absorption band with $\lambda_{max} \simeq 670$ nm, while the final spectrum exhibits two absorption bands in this region with $\lambda_{max} \simeq 635$ and $\simeq 679$ nm. (d) Inset D shows the time course at 672 nm. These two long wavelength spectral bands in the final spectrum are derived from d-d transitions in the Co(II)-E(NAD–pyrazole) complex (Maret, 1980). It is evident from a comparison of the two time courses that the decay of the intermediate and the changes in the d–d spectral bands (within the limits of experimental error) occur with the same rate. (e) Figure 5E shows the set

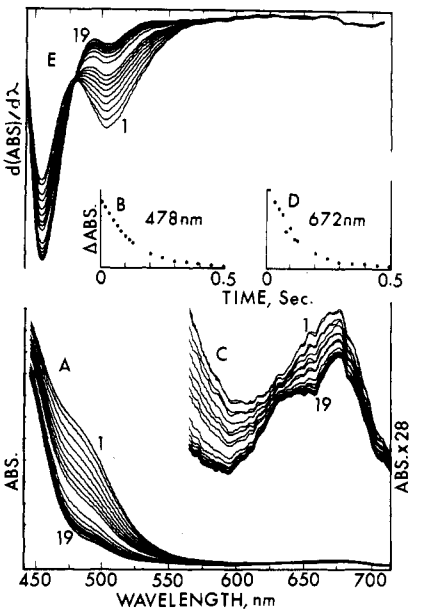

FIGURE 5: Time-resolved spectra (A; C), single wavelength time courses (B; D), and derivative spectra (E) for intermediate decay with the Co(II)-substituted enzyme from the rapid scanning spectrophotometer. The spectra in (A) record the disappearance of the intermediate (λ_{max} 478 nm). The intense absorbance at 450 nm is primarily due to the large excess of DACA. The spectra in (C) record (on a 28× expanded scale; right ordinate) the changes in the Co(II) d–d transitions in the 600–700-nm region. The sequences of the 19 traces in (A), (C), and (E) are indicated by the numbers shown. The absorbance changes during intermediate decay at 478 and 672 nm are shown in (B) and (D), respectively. The first-derivative spectra, $dA/d\lambda$, are shown in (E). The first-derivative spectra were calculated by using the method of Savitzsky & Golay (1964) with a bandwidth of 9 nm. Due to the high frequency noise apparent in (C), meaningful derivative spectra could not be obtained in the 600–700-nm region. Conditions: [Co(II)-E] = 21.5 μN; [NADH] = 42.8 μM; [DACA] = 75 μM; [pyr] = 20 mM; 0.05 M sodium acetate buffer, pH 4.4; 25.0 ± 0.2 °C.

of first-derivative spectra (with respect to wavelength). These spectra are notable for the intersection point located at 478 nm.[2]

Discussion and Conclusions

The herein presented transient kinetic investigations of the LADH catalytic mechanism provide direct measures of the effects of the substitution of Co(II), Ni(II), and Cd(II) for Zn(II) at the LADH site on some of the physical and chemical events occurring during catalysis. Because the experimental conditions employed limit reaction to a single turnover of sites, individual processes in the mechanism can be isolated and studied in the absence of the kinetic complications associated with multiple turnovers.

Formation of the DACA intermediate occurs in a rapid, reversible, and pH-independent step between pH 4 and pH 10 (Scheme I). The decay of the intermediate (under single-turnover conditions) is markedly pH dependent (Figure 2). At low pH, this decay process is subject to a primary kinetic isotope effect when NADD is substituted for NADH.

[2] If $dAbs/d\lambda$ = constant with respect to time at some wavelength, then any change by one reacting species must be exactly compensated for by the changes in all other species at that wavelength. This places limits on the location of intersection points for two interconverting species; if an absorber is converted to a nonabsorbing species, the interaction point must be located at the λ_{max} of the absorber. For two interconverting absorbers, any intersection points will occur red shifted from the longer wavelength absorber and blue shifted from the shorter wavelength absorber.

No isotope effect is observed at high pH (Figure 2 and Table I). As already shown for the native Zn(II)-enzyme (Morris et al., 1980), the data presented in Figures 2 and 3 establish that the decay of the enzyme-bound DACA intermediate, designated (NADH)E(I) in Scheme II, undergoes a change in rate-limiting step from hydride transfer at low pH to a subsequent step in the mechanism at high pH. The rate-limiting step at high pH is proposed to involve release of product from the site (Morris et al., 1980) according to the mechanism outlined in Scheme II:

Scheme II

$$(\text{NADH})\text{E(I)} \underset{k_{-1}}{\overset{k_1}{\rightleftharpoons}} (\text{NAD}^+)\text{E(P)} \quad (6)$$

$$(\text{NAD}^+)\text{E(P)} + \text{H}^+ \underset{k_{-2}}{\overset{k_2}{\rightleftharpoons}} (\text{NAD}^+)\text{E(P)(H}^+) \quad (7)$$

$$K_a = k_{-2}/k_2$$

$$(\text{NAD}^+)\text{E(P)(H}^+) \underset{k_{-3}}{\overset{k_3}{\rightleftharpoons}} \text{E(NAD}^+) + \text{PH} \xrightarrow[k_4]{\text{pyr}} \text{E(NAD–pyr)} \quad (8)$$

With the assumption that (a) the Bodenstein steady-state approximation is valid for the product of step 6, (b) that equilibrium greatly favors (NADH)E(I) in step 6 (Dunn & Hutchison, 1973), (c) that step 7 (where $K_a = k_{-2}/k_2$) is in mobile equilibrium, and (d) that step k_3 is quasi-irreversible (i.e., $k_4[\text{pyr}] \gg k_{-3}$), the rate expression for this mechanism (Morris et al., 1980) is given by

$$\text{rate} = \frac{-\text{d}[(\text{NADH})\text{E(I)}]}{\text{d}t} = \frac{k_1[(\text{NADH})\text{E(I)}][\text{H}^+]}{K_a(k_{-1}/k_3) + [\text{H}^+]} \quad (9)$$

When $[\text{H}^+] \ll K_a(k_{-1}/k_3)$, eq 9 reduces to

$$v \simeq \frac{k_1k_3[(\text{NADH})\text{E(I)}][\text{H}^+]}{K_ak_{-1}} \quad (10)$$

and the observed rate constant will be subject only to the equilibrium isotope effect for hydride transfer [a value near unity (Morris et al., 1980; Cook et al., 1980)] when NADD is substituted for NADH.

When $[\text{H}^+] \gg K_a(k_{-1}/k_3)$, eq 9 reduces to

$$v \simeq k_1[(\text{NADH})\text{E(I)}] \quad (11)$$

Equation 11 predicts that hydride transfer will become rate limiting at low pH, and therefore, the observed rate constant will be subject to a primary kinetic isotope effect. The data presented in Figures 2 and 3 and Table I are fully consistent with these predictions.

In the rapid-scanning experiments (Figure 5), two chromophoric probes of the chemical reaction are under observation: the intense 478-nm absorption of the coordinated intermediate and the d–d transition of the active-site cobalt ion. Since changes in the 600–700-nm region are the result of different environments of Co(II), the changes in the d–d spectral bands provide additional information about transformations at the site. As both these probes detect a single and identical phase (Figure 5), we conclude that the only stoichiometrically significant species observed in the decay process are the DACA intermediate and E(NAD-pyr). This conclusion is supported by the presence of an intersection point at 478 nm in the set of first-derivative spectra (Figure 5E). Such an intersection point at the maximum of a known intermediate implies that there can be no buildup and disappearance of another chromophoric species in significant amounts in the 440–540-nm region during the decay phase of the reaction.[2]

Nature of the Hydride Transfer Transition State. The rate constants for the hydride transfer process (k_H values, Table I) obtained for the Zn(II)-, Co(II)-, and Ni(II)-enzymes are very similar, while the value for the Cd(II)-enzyme is much smaller. The Zn(II)-, Co(II)-, and Ni(II)-enzymes yield the same kinetic isotope effect ($k_H/k_D \simeq 2.8$–3.1). The isotope effect for the Cd(II)-enzyme appears to be slightly smaller with $k_H/k_D \simeq 1.7$. These observations lead us to conclude that for the Zn(II)-, Co(II)-, and Ni(II)-enzymes, the nature of the transition state for hydride transfer is almost unchanged by these metal ion substitutions. The ~40-fold decrease in k_H for the Cd(II)-enzyme relative to the Zn(II) enzyme and the lower kinetic isotope effect indicate that substitution of Cd(II) for Zn(II) alters the transition state for hydride transfer.

Analysis of λ_{max}, $\Delta\lambda_{max}$, k_H, k_{on}, and k_{off}. Previous investigations of the influence of Lewis acid strength on the spectra of DACA and DACA analogues (Angelis et al., 1977) show a rough correlation between the expected strength of the Lewis acid and the magnitude of the red shift. For example, bonding of the carbonyl of DACA to Zn(II), Sn(IV), and $C_2H_5^+$ results in $\Delta\lambda_{max}$ values of 64, 85, and 110 nm, respectively. Coordination of the DACA analogue, *trans*-4-(*N*,*N*-dimethylamino)cinnamaldehyde 1′-pyridinohydrazone (II) to Co^{2+}, Zn^{2+}, Ni^{2+}, and Cd^{2+} (Angelis et al., 1977) gives a much smaller range of red shifts: 56, 52, 39, and 42 nm (unpublished experiments), respectively.

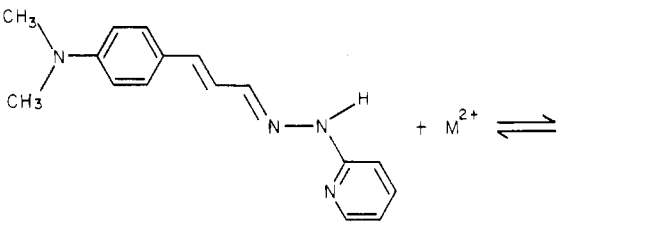

II

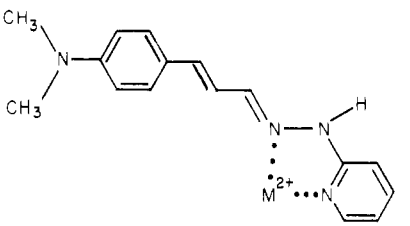

III

The lack of an exact correspondence between the spectral shifts reported for the complexes with II and the spectral shifts observed for the DACA intermediate (Table I) almost certainly is due to a variation in coordination number and geometry in the model complexes that is absent in the enzyme complexes. The zinc complex with II is tetrahedral (Angelis et al., 1977), the cobalt complex probably is tetrahedral, the nickel complex probably is square planar (Holm & O'Connor, 1971), and the cadmium complex probably has a coordination greater than 4 (Cotton & Wilkinson, 1980).

If the magnitude of the spectral shift reflects the strength of the bonding interaction between DACA and the active-site metal, then there also should be correlations between the magnitude of the spectral shift, k_H, k_{off}, and K_d. The close similarities in spectral shifts predict close similarities in Lewis acid strengths with the order of strengths expected to be Co(II)-E > Ni(II)-E ≥ Zn(II)-E > Cd(II)-E. The order of

reactivity as measured by k_H, i.e., Co(II) > Zn(II) ≃ Ni(II) ≫ Cd(II), roughly parallels the expected relative Lewis acid acidities of these metal ions in a tetrahedral ligand field (Schläfer & Gliemann, 1967). However, when compared with the other derivatives, the $\Delta\lambda_{max}$ value for the Cd(II)-enzyme appears too large in relation to the rate of hydride transfer. The data in Table I show that both k_{off} and K_d decrease with increasing $\Delta\lambda_{max}$. This trend is expected if the variations in k_{off} and K_d are determined by the variations in the strength of the bonding interactions between DACA and the metal ion.

Our previous work indicates that the rate of formation of the DACA intermediate is limited either by diffusion or by displacement of inner sphere coordinated water (Dunn & Hutchison, 1973; Koerber et al., 1980). The values of k_{on} and k_{off} are independent of pH between pH 4 and pH 10 (Dunn & Hutchison, 1973; Dunn et al., 1975; Morris et al., 1980). Andersson et al. (1981) have found that the value of K_d for DACA increases above pH 10 and depends upon an apparent $pK_a \simeq 11.2$. Although other explanations are possible, this finding suggests that the ionization of zinc-bound water interferes with DACA binding and that displacement of zinc-coordinated hydroxide ion becomes rate limiting for intermediate formation at high pH. Below pH 10, the insensitivity of k_{on} to the nature of the metal ion (Table I) is more consistent with a diffusion-limited rate of association than with a rate-limiting dissociation of water.

The simplest mechanism for the formation of the DACA intermediate consists of a diffusion-limited reaction in which DACA becomes coordinated to the active-site metal ion via a pentacoordinate species as shown in eq 12.

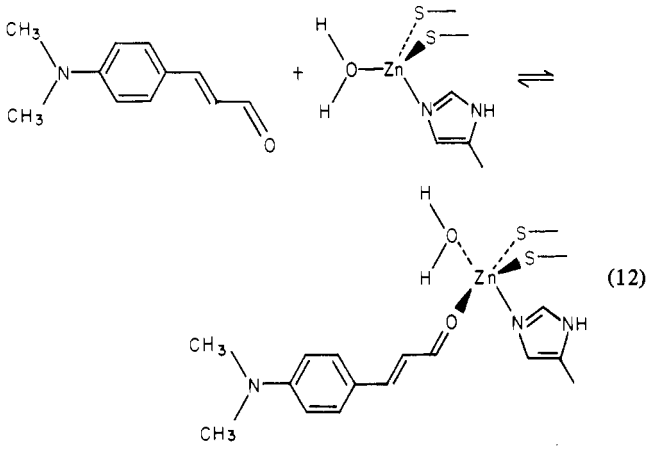

(12)

The available structural and kinetic data are insufficient to determine whether or not the water molecule is released in a subsequent fast step. X-ray data for the Zn(II)-E-(H_2NADH)(DACA)[1] complex indicates a warped tetrahedral ligand field for zinc ion (E. Zeppezauer, personal communication), suggesting that the release of water occurs.

Dependence of pK_{app} on Metal Ion. Previous work (Morris et al., 1980) with the Zn(II)-enzyme shows the presence of a deuterium kinetic isotope effect on K_{app} when NADD is substituted for NADH. Because $K_{app} = K_a(k_{-1}/k_3)$, viz., eq. 9, this isotope effect was proposed to reflect a primary kinetic isotope effect on k_{-1}, and k_{-1}^H/k_{-1}^D was estimated to be ≃3.0 (for a $pK_{app}^D - pK_{app}^H \simeq 0.5$). The data summarized in Table I show similar shifts in pK_{app} when NADD is substituted for NADH. From these data it is evident that for the Zn(II)-, Co(II)-, and Ni(II)-enzyme species, $k_{-1}^H/k_{-1}^D \simeq 3.0$. Although the pH dependencies for the Cd(II)-enzyme appear similar (Figure 3), a quantitative treatment of the rate data for this derivative to determine pK_{app} values was not justified by the quality of the rate data.

Table I also shows a regular dependence of pK_{app} on the nature of the active-site metal ion, with pK_{app} decreasing with increasing Lewis acid strength. Since K_{app} is a complex quantity, the dependence of pK_{app} on metal ion could be complicated. The variation in pK_{app} may reflect changes in the microscopic pK_a of the ionizable group responsible for the pH dependence of the decay process. According to Scheme II, this process could be either the ionization of a metal-coordinated species (i.e., alcohol) or the ionization of an enzyme residue that regulates product release. The data presented in Table I indicate that within the LADH active site Zn(II), Co(II), and Ni(II) exhibit similar Lewis acid strengths; consequently, it is not surprising that the pK_{app} values for these derivatives vary over only a small range (i.e., from ≃5.5 to ≃6.0). Substitution of Cd(II) for Zn(II) is expected to cause a larger perturbation. Unfortunately, a quantitative measure of pK_{app} for the Cd(II)-enzyme (Figure 3) could not be obtained.

Theoretical Expectations. The substitution of chemically and spectroscopically interesting divalent metal ions for zinc ion has been accomplished for a wide variety of zinc metalloproteins [see Lindskog et al. (1971), Lindskog (1970), Dunn (1975), Coleman (1971), and Maret et al. (1979)]. Substitution of Co(II) generally results in the retention of high catalytic activity in zinc metalloenzymes (Lindskog, 1970; Dunn, 1975). The substitution of other divalent metal ions (such as Ni^{2+}, Mn^{2+}, Fe^{2+}, Cu^{2+}, and Cd^{2+}) has been useful in specific instances.

The literature concerning metal ion catalysis in small molecule systems is of limited assistance in the detailed interpretation of the effects of metal ion substitutions in metalloenzymes. Although the kinetic consequences of metal ion substitution frequently have been studied, rarely have those studies been accompanied by a rigorous determination of the coordination numbers and geometries of the reacting complexes as a function of the metal ion involved. Consequently, the relative differences in catalytic effectiveness of divalent metal ions is not well understood. Due to constraints imposed by protein ternary and quaternary structure, it may be that the roles played by metal ions in catalysis are more easily studied via metal ion substituted enzymes than via small molecule complexes. Structural constraints built into the enzyme are more likely to ensure consistency in coordination number, geometry, and the alignment of reacting atoms, thus maintaining similarities in transition states from metal ion to metal ion. Such consistency cannot be expected in most small molecule systems.

The rich literature pertaining to selected small molecule metal complexes provides overlapping sets of data sufficient to predict the Lewis acid characters of tetrahedral Zn(II), Co(II), Ni(II), and Cd(II) from physical, chemical, and structural data. A review of selected X-ray structures for tetrahedral Zn(II), Co(II), and Ni(II) complexes with the same ligands shows the metal–ligand bound distances for nitrogen and oxygen ligands to be essentially identical (±0.01 Å), and in numerous examples the crystals are isomorphous (Lundberg, 1966; Antti & Lundberg, 1972; Horrocks et al., 1980; Sacconi et al., 1962; Sacconi & Orioli, 1962; Holm & O'Connor, 1971). In tetrahedral mercaptide complexes, the Zn–S and Co–S distances are nearly identical (2.34 vs. 2.32 Å) while the Ni–S distance is slightly shorter (2.29 Å), reflecting a more distorted tetrahedral ligand field. The Cd–S distance is considerably longer (2.54 Å) (Swenson et al., 1978). Clearly, the replacement of the LADH active-site zinc ions by Co(II) represents a structurally conservative substitution.

Scheme III: Structural Representation of the Liver Alcohol Dehydrogenase Active Site Comparing Bonding Details for the Zn(II)- and Cd(II)-E Intermediates[a]

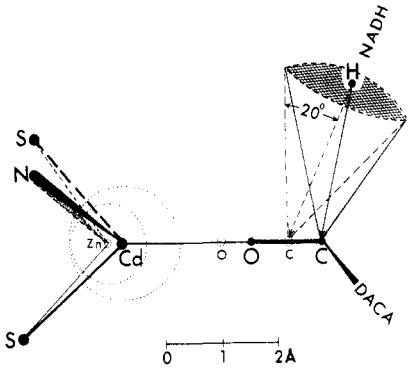

[a] The assumptions upon which this model is based are given in the text. The solid dots show the positions of the carbonyl of DACA and the active-site cadmium ion for the Cd(II)-E. In this model, the position of the (4*R*)-4-hydrogen of NADH is restricted to the crosshatched circular surface (defined by the cone) located at the van der Waals distance from the carbonyl carbon. The small dotted circles show the positions of the DACA carbonyl and zinc ion for the Zn(II)-E. The large dotted circles represent the ionic radii of Zn^{2+} (≃0.70 Å) and Cd^{2+} (≃1.0 Å). The arrows show how the distances between the (4*R*)-hydrogen and the carbonyl carbon would change upon replacement of Zn(II) by Cd(II). The bond lengths used to construct the drawing are based on typical values from X-ray crystallographic studies involving small molecule analogues.

The literature on four-coordinate Ni(II) complexes shows that, unless steric constraints interfere, Ni(II) prefers to form square-planar complexes (Holm & O'Connor, 1971). However, the difference in energy between tetrahedral and square-planar coordination is small, and a number of square-planar ⇌ tetrahedral interconverting systems have been found [see Holm & O'Connor (1971)]. If it is assumed that covalent forces and van der Waals contacts constrain the site ligands (Brändén et al., 1976), then the Ni(II) derivative also should be isomorphous to the zinc enzyme. Although five-coordinate structures cannot be ruled out, the UV–visible spectra and CD spectra of the Co(II)- and Ni(II)-enzymes both are consistent with distorted tetrahedral coordination geometries (Dietrich et al., 1981, 1979; Maret et al., 1979).

In contrast, the more polarizable character and the much larger ionic radius of Cd^{2+} (≃1.0 Å vs ≃0.7 Å for Zn^{2+}) results in correspondingly longer bond lengths and coordination numbers > 4. Tetrahedral Cd(II) complexes are rare. Therefore, it is not obvious that the Cd(II)-substituted enzyme is tetrahedral. If the Cd(II)-enzyme is tetrahedral, bonds to cadmium will be 0.2–0.3 Å longer than to the other enzyme derivatives. The bonds to cadmium will be even longer for coordination numbers > 4. The larger ionic radius and consequent longer bond lengths make Cd(II) a weaker Lewis acid than Zn(II), Co(II), or Ni(II).

If an approximately tetrahedral ligand field is assumed for both Zn(II) and Cd(II), then the structures in Scheme III compare active-site dimensions for the two intermediates. The Cd(II) structure has been constructed by assuming that (1) the coordinates of Cys-46, His-67, Cys-174, and the nicotinamide ring of NADH do not change, (2) the bond lengths found in the tetrahedral small molecule complexes are appropriate, (3) the hydrogen at the 4 position of the nicotinamide ring is in van der Waals contact with the carbonyl carbon of DACA in the Zn(II)-enzyme complex, (4) Zn(II) and Cd(II) have ionic radii of 0.70 and 1.0 Å, respectively, (5) upon substitution of Cd(II) for Zn(II), the carbonyl of DACA is simply displaced along the metal–oxygen bond axis (i.e., there is no rotational or angular displacement of DACA), and (6) hydride transfer in the Zn(II)-enzyme occurs through a linear transition state. Theoretical models (Williams et al., 1980; Bürgi et al., 1974) indicate the most likely direction for nucleophilic attack on a carbonyl occurs in a plane perpendicular to the plane of the carbonyl group along a line which forms a $H^-\cdots C{=}O$ bond angle of approximately 109° (the tetrahedral angle). In accord with intuition, the model calculations indicate that for a separating distance of ~3 Å (i.e., van der Waals contact), large deviations from the tetrahedral angle (±20°) cause negligible increases in the energy of the system. Thus, if the actual approach of hydride is assumed to lie within the cone produced by rotation of a line subtended from the carbonyl carbon at an angle of 20° about the tetrahedral approach axis (viz., Scheme III), then for the constellation of atoms shown in Scheme III, the longer bonds to cadmium would have little effect on the distance between the (4*R*)-4-hydrogen of NADH and the carbonyl carbon of DACA. Depending on the exact location of the (4*R*)-4-hydrogen within the cone, the distance to the carbonyl carbon could increase, decrease or remain unchanged upon substitution of Cd(II) for Zn(II). The extremes defined by the cone indicate changes in distance of ~+0.2 Å (for a $H^-\cdots C{-}O$ angle of 89°) to ~–0.2 Å (for a $H^-\cdots C{-}O$ angle of 129°).

It seems improbable to us that the 40-fold slower rate of hydride transfer exhibited by the Cd(II)-enzyme could be explained by the ±0.2-Å change in distance predicted by Scheme III. However, the change in rate could be accounted for if, upon substitution of Cd(II) for Zn(II), DACA undergoes rotation and/or angular displacement. Rotation and/or angular displacement could result either from restrictive van der Waals contacts between DACA and the site or from a coordination number different from the Zn(II) complex. Any such change in orientation would bring about the misalignment of the reacting atoms, thereby increasing the activation energy for hydride transfer. This misalignment would also explain the inexact correspondence between the rate of hydride transfer and $\Delta\lambda_{max}$ (Table I).

On the basis of the foregoing considerations, we conclude that the close similarities in the rates of hydride transfer (Table I) for the Zn(II)-, Co(II)-, and Ni(II)-enzymes is a consequence of similar Lewis acid strengths.[3] The lower reactivity and the smaller kinetic isotope effect of the Cd(II)-enzyme could arise from one or more factors: (a) Due to the undoubtedly longer Cd–O bond length to DACA, the Cd(II)-enzyme is expected to be less effective in activating the carbonyl of DACA in the hydride transfer step. (b) The tendency of cadmium to form complexes of coordination number > 4 makes the assignment of coordination less certain. (c) The longer bonds to Cd(II) could result in slight misalignments of the reacting atoms, thereby increasing the activation energy for reaction and altering the transition state with respect to bond scission and formation during hydride transfer. Since the Zn(II), Co(II), and Ni(II) derivatives yield similar kinetic isotope effects, rate constants, and pH dependencies for the process of intermediate decay, we conclude that the transition states and therefore the structures of the activated complexes are highly similar. Consequently, the 40-fold smaller hydride transfer rate and the slightly smaller kinetic isotope effect of the Cd(II)-enzyme reflect the effects (both electronic and

[3] Our preliminary results (A. K. H. MacGibbon, H. Dietrich, M. Zeppezauer, and M. F. Dunn, unpublished experiments) indicate that these metal ion substitutions exert larger effects on coenzyme dissociation rates.

steric) of the small structural perturbation introduced by the ≥0.3-Å increase in the ionic radius of Cd(II) over Zn(II). These effects perturb the activation energy for hydride transfer. The apparent decrease in isotope effect suggests the position of the transition state relative to hydride transfer also has been perturbed.

References

Andersson, I. (1980) Dissertation, Universität des Saarlandes, Saarbrücken, West Germany.

Andersson, P., Kvassman, J., Lindström, A., Oldén, B., & Pettersson, G. (1981) *Eur. J. Biochem. 113*, 425–433.

Angelis, C. T., Dunn, M. F., Muchmore, D. C., & Wing, R. M. (1977) *Biochemistry 16*, 2922–2931.

Antti, C.-J., & Lundberg, B. K. S. (1972) *Acta Chem. Scand. 26*, 3995–4000.

Bernasconi, C. F. (1976) in *Relaxation Kinetics*, p 13, Academic Press, New York.

Bobsein, B. R., & Myers, R. J. (1980) *J. Am. Chem. Soc. 102*, 2454–2455.

Brändén, C.-I., Jörnvall, H., Eklund, H., & Furugren, B. (1976) *Enzymes, 3rd Ed. 2A*, 103–190.

Bürgi, H. B., Lehn, J. M., Wipff, G. (1974) *J. Am. Chem. Soc. 96*, 1956–1957.

Coleman, J. E. (1971) *Progr. Bioorg. Chem. 1*, 311–317.

Cook, P. F., Blanchard, J. S., & Cleland, W. W. (1980) *Biochemistry 19*, 4853–4858.

Cotton, F. A., & Wilkinson, G. (1980) in *Advanced Inorganic Chemistry*, 4th ed., pp 597–602, Wiley, New York.

Coutts, S. M., Riesner, D., Römer, R., Rabl, C. R., & Maass, G. (1975) *Biophys. Chem. 3*, 275–289.

Dalziel, K. (1957) *Acta Chem. Scand. 11*, 397–398.

Dietrich, H. (1980) Dissertation, Universität des Saarlandes, Saarbrücken, West Germany.

Dietrich, H., Maret, W., Wallén, L., & Zeppezauer, M. (1979) *Eur. J. Biochem. 100*, 267–270.

Dietrich, H., Maret, W., Kozlowski, H., & Zeppezauer, M. (1981) *J. Inorg. Biochem. 14*, 297–311.

Drum, D. E., & Vallee, B. L. (1970) *Biochem. Biophys. Res. Commun. 41*, 33–39.

Dunn, M. F. (1975) *Struct. Bonding (Berlin) 23*, 61–122.

Dunn, M. F., & Hutchison, J. S. (1973) *Biochemistry 12*, 4882–4892.

Dunn, M. F., Biellmann, J.-F., & Branlant, G. (1975) *Biochemistry 14*, 3176–3182.

Dunn, M. F., Bernhard, S. A., Anderson, D., Copeland, A., Morris, R. G., & Roque, J.-P. (1979) *Biochemistry 18*, 2346–2354.

Holm, R. H., & O'Connor, M. J. (1971) *Prog. Inorg. Chem. 14*, 241–401.

Horrocks, W. D., Ishley, J. N., Holmquist, B., & Thompson, J. S. (1980) *J. Inorg. Biochem. 12*, 131–141.

Jencks, W. P. (1969) in *Catalysis in Chemistry and Enzymology*, pp 577–585, McGraw-Hill, New York.

Koerber, S. C., & Dunn, M. F. (1981) *Biochimie 63*, 97–102.

Koerber, S. C., Schack, P., Au, A. M.-J., & Dunn, M. F. (1980) *Biochemistry 19*, 731–738.

Lindskog, S. (1970) *Struct. Bonding (Berlin) 8*, 153–196.

Lindskog, S., Henderson, L. E., Kannan, K. K., Liljas, A., Nyman, P. O., & Strandberg, B. (1971) *Enzymes, 3rd Ed. 5*, 587–665.

Lundberg, B. K. S. (1966) *Acta Crystallogr. 21*, 901–909.

Maret, W. (1980) Dissertation, Universität der Saarlandes, Saarbrücken, West Germany.

Maret, W., Andersson, I., Dietrich, H., Schneider-Bernlöhr, H., Einarsson, R., & Zeppezauer, M. (1979) *Eur. J. Biochem. 98*, 501–512.

Maret, W., Dietrich, H., Ruf, H. H., & Zeppezauer, M. (1980) *J. Inorg. Biochem. 12*, 241–252.

McFarland, J. T., & Bernhard, S. A. (1972) *Biochemistry 11*, 1486–1493.

Morris, R. G., Saliman, G., & Dunn, M. F. (1980) *Biochemistry 19*, 725–731.

Rafter, G. W., & Colwick, S. P. (1957) *Methods Enzymol. 3*, 887.

Sacconi, L., & Orioli, P. L. (1962) *Ric. Sci. 32*, 645.

Sacconi, L., Orioli, P. L., Paoletti, P., & Ciampolini, M. (1962) *Proc. Chem. Soc., London*, 255–256.

Savitzsky, A., & Golay, M. J. E. (1964) *Anal. Chem. 36*, 1627–1639.

Schläfer, H. L., & Gliemann, G. (1967) Einfurhrung in die Ligandenfeldtheorie Akademische Verlagsgesellschaft, Frankfurt.

Shore, J. D., & Gutfreund, H. (1970) *Biochemistry 9*, 4655–4659.

Shore, J. D., & Santiago, D. (1975) *J. Biol. Chem. 250*, 2008–2012.

Silverman, E. (1965) *Anal. Biochem. 12*, 199–212.

Sund, H., & Theorell, H. (1963) *Enzymes, 2nd Ed. 7*, 25–83.

Swenson, D., Baenziger, N. C., & Coucouvanis, D. (1978) *J. Am. Chem. Soc. 100*, 1932–1934.

Sytkowski, A. J., & Vallee, B. L. (1978) *Biochemistry 17*, 2850–2857.

Theorell, H., & Yonetani, T. (1963) *Biochem. Z. 338*, 537.

Williams, I. H., Maggiora, G. M., & Schowen, R. L. (1980) *J. Am. Chem. Soc. 102*, 7831–7839.